Overall Kinetics of Heterogeneous Elemental Mercury Reactions on TiO_2 Sorbent Particles with UV Irradiation

Tai Gyu Lee

Department of Chemical Engineering, Yonsei University, 134 Sinchon-dong, Seodaemun-gu, Seoul 120-749, Korea

Pratim Biswas*

Environmental Engineering Science Division, Departments of Chemical and Civil Engineering, Campus Box 1180, Washington University at St. Louis, St. Louis, Missouri 63130-4899

Elizabeth Hedrick

National Exposure Research Laboratory, U.S. Environmental Protection Agency, Cincinnati, Ohio 45268

The kinetics of gas-phase elemental mercury (Hg^0) oxidation on titania particle surfaces in the presence of UV irradiation was established. Overall reaction orders with respect to the gas-phase mercury concentration (α) and the UV intensity (β) were found to be 1.4 ± 0.1 and 0.35 ± 0.05 for the differential bed reactor, whereas values of α and β were 1.1 ± 0.1 and 0.39 for the aerosol flow reactor (AFR). While the values are similar, the AFR results are more representative of the practical sorbent process. In the low-temperature range (<80 °C), the overall rate of initial mercury uptake increased as the temperature increased, indicating that it was a reaction-controlled process. At higher temperatures (>110 °C), an increase of the temperature resulted in a decrease of the overall reaction rate, indicating an adsorption-controlled process.

1. Introduction

Mercury, 1 of the 11 trace metals (As, Be, Cd, Co, Cr, Hg, Mn, Ni, Pb, Sb, and Se) whose emission control is currently being stipulated by the U.S. Environmental Protection Agency (EPA) under Title III of the 1990 Clean Air Act Amendments, possesses unique characteristics, such as high volatility, a tendency to bio-accumulate, and toxic properties. The major anthropogenic sources of the mercury emissions are coal combustors and municipal waste incinerators. Unlike most other trace metals that are emitted in particulate forms, mercury has been reported to be released in vapor-phase elemental form, which is not effectively captured in typical air pollution control devices.[1]

A novel control methodology wherein a titania sorbent precursor is injected into the combustor has been proposed for the capture of elemental mercury.[2] In situ generated sorbent particles in a flow reactor system, compared to traditional bulk types used in a fixed or fluidized bed, have been shown to possess a higher metal capture efficiency[3−5] as well as to suppress the formation of submicrometer particles,[3] resulting in lower emissions. The mechanistic pathway of the elemental mercury capture process is illustrated in Figure 1. The precursor injection conditions are selected so that a highly agglomerated structure consisting of nanometer-sized (20−30 nm) titania particles is formed. This high surface area open-structured agglomerate allows effective irradiation by UV light and minimal mass-transfer resistance for the elemental Hg species. Thus, a low ratio of Ti sorbent to elemental Hg is effective in obtaining high capture efficiencies.[2]

Several researchers studied the quantitative evaluation of kinetic parameters, such as the reaction order and rate constant for heterogeneous gas−solid photocatalytic reactions. Some fitted their kinetic data to the Langmuir−Hinshelwood (LH) expression[6−8] and evaluated the kinetic parameters, while Dibble and Raupp[9] tried to evaluate the kinetic parameters using the integral rate law expression. Differential bed reactor (DBR) systems have been used conventionally for kinetic studies of the heterogeneous gas−solid reaction. Fan and co-workers[10−12] studied the reaction kinetics of toxic metals (such as arsenic and selenium) removal by Ca-based sorbents using differential fixed-bed reactors. The two important factors that govern the rate of gas−solid reactions are the surface reaction rate and the external mass-transfer rate. DBR systems minimize the external mass-transfer resistance, thus providing information solely on the surface reaction rate. Although there have been several studies on the reactions between titania and organics or other sorbents and inorganics, there are relatively few kinetic studies on the photocatalytic reaction of titania with inorganic compounds in the gas phase (or suspended aerosol phase). Determining kinetic constants in entrained-flow reactor studies is important because toxic metal capture (such as mercury) in practical systems such as coal combustors and incinerators will be by injection of sorbents in the exhaust gas streams.

In this paper, the overall kinetics of elemental mercury (Hg^0) uptake by TiO_2 in the presence of UV irradiation is reported. Two reactor systems were used: a DBR and an aerosol flow reactor (AFR). The data from the two different systems were collected, analyzed, and then compared to establish the kinetic parameters of elemental Hg uptake by TiO_2 in the presence of UV irradiation.

* To whom correspondence should be addressed. Tel.: (314)-935-5482. Fax: (314)935-5464. E-mail: pratim.biswas@wustl.edu.

10.1021/ie0303707 CCC: $27.50
Published on Web 02/19/2004

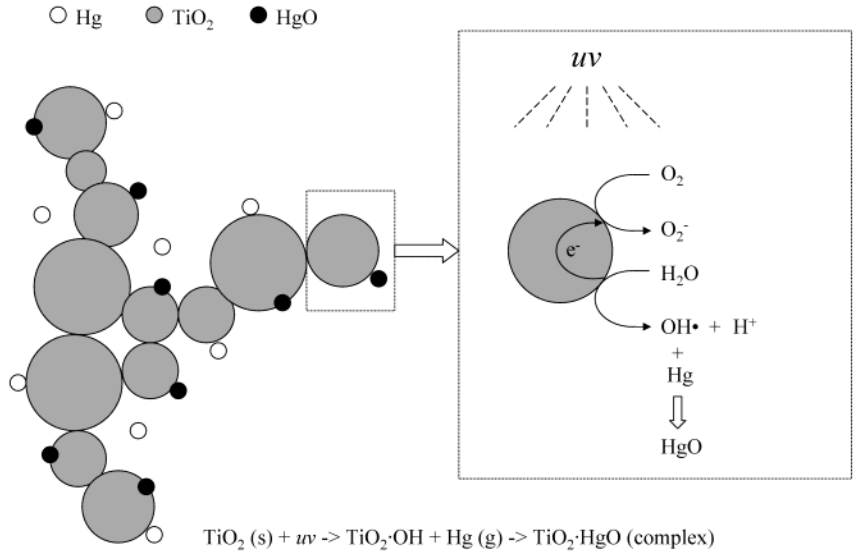

Figure 1. Mechanistic description of Hg^0 capture by TiO_2 in the presence of UV irradiation.

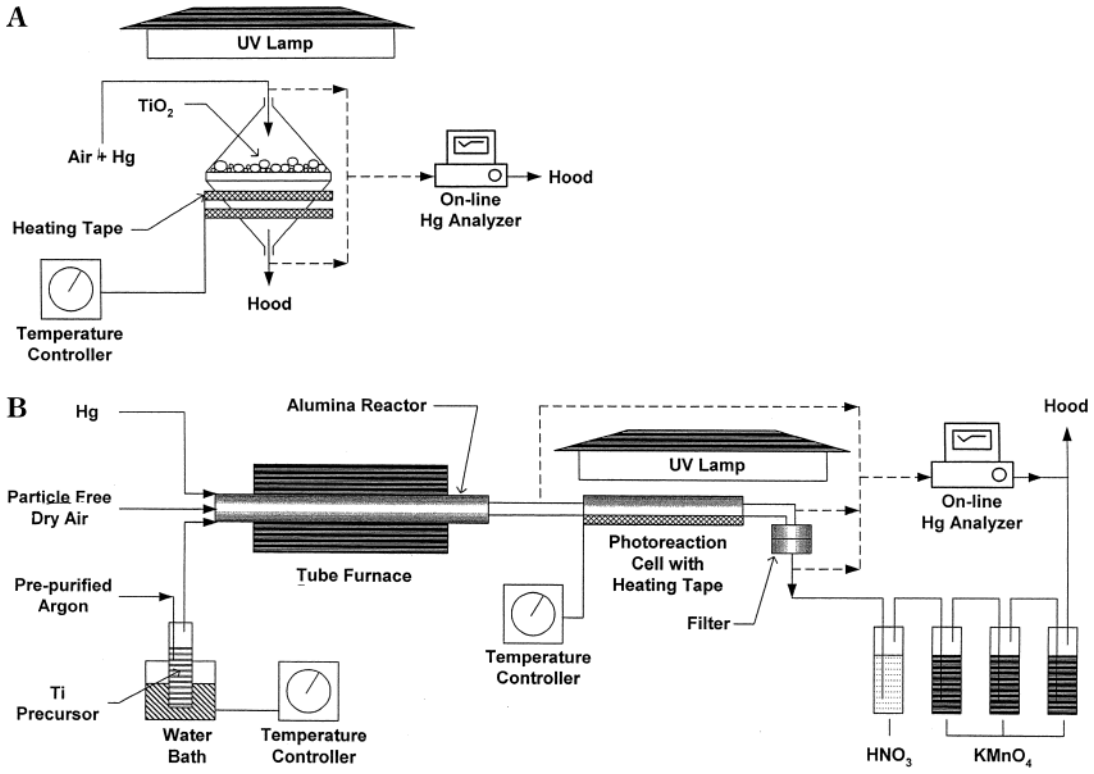

Figure 2. (A) Schematic diagram of the DBR system. (B) Schematic diagram of the AFR system.

2. Experimental Section

2.1. DBR System. The schematic diagram of the fixed-bed-type reactor to study mercury reaction rates is shown in Figure 2A. The TiO_2 particles were placed on the glass fiber filter, which was located in a filter holder (Filter Support 7519, ACE Glass Inc.) made from UV-transmittable glass (borosilicate). The filter holder was placed under UV lamps and irradiated with 354 nm UV light. Compressed air was passed through a high-efficiency particulate air filter and air cleaner (75-62 FT-IR purge gas generator, Balston Filter Products) to ensure that it was particle free. Mercury vapor was introduced into the system by passing particle-free air at a precisely controlled flow rate (MKS Mass-Flo Controller, MKS Instruments, Inc.) above liquid mercury contained in a temperature-controlled gas washing bottle. The gas stream was then sent to the online mercury analyzer for real-time monitoring of the elemental mercury concentration in the gas phase. The online analyzer (modified Shimadzu UV-1201S spectrometer) was calibrated using a modified U.S. EPA Method 29[13] with cold vapor atomic absorption analysis.[14−16] The bottom half of the glass filter holder was covered with heating tape so that the temperature inside could be varied. The temperature was controlled with a power controller (type 45500, Thermolyne). Only the bottom half was covered to allow UV light to penetrate through the top half of the filter holder.

Two types of titania powders were used: commercially available (Degussa P25, Degussa Corp.) and aerosol-route-generated titania agglomerates.[14,16,17] The commercial titania powders were spherical, nonporous, and

Table 1. Description of the Experimental Plans and Conditions[a]

system	type of TiO_2 used	mass of TiO_2 used (g)	air flow rate through a Hg feed bottle (cm^3/min)	precursor inlet bubbler temp (°C)	Ar flow rate through a Ti precursor bubbler (cm^3/min)	UV intensity ($\mu W/cm^2$) × 10^2	photochemical reaction temp (°C)
DBR	Degussa P25	0.001, 0.005, 0.01	20, 30, 40, 50			0, 0.475, 2.18, 4.73, 9.83	24, 50, 60, 70
	aerosol route generated	0.001					
AFR	in situ generated		2, 4, 6, 8, 10, 12	75	200	0, 1.28, 4.33, 11.4, 25.6	24, 40, 50, 80, 110, 130
				85	200−300		

[a] Total flow rate in the system = 1 L/min.

primarily the anatase phase and had a measured Brunauer−Emmett−Teller (BET) surface area of ~50 m^2/g (model ASAP2000, Micrometrics). The aerosol-reactor-synthesized titania (oxidation of titanium isopropoxide at 1000 °C) consisted of an agglomerate of nanosized primary particles. The BET surface area was 64.5 ± 0.5 m^2/g, and the crystalline phase was purely anatase. Table 1 shows the matrix of the experimental plans for the DBR system. The masses of the TiO_2 powder used were 0.001, 0.005, and 0.01 g for Degussa P25 and 0.001 g for the aerosol-route-generated ones. The range of Hg inlet concentrations tested was 1.0−10.0 $\mu g/m^3$.

Metal screens of different meshes were placed right below the UV lamp used to vary the UV intensity through the filter holder onto the TiO_2 powders. The UV intensities measured by a UV radiometer with a microprocessor (UVImeter RX003, UVItec) inside the filter holder were 4.75 × 10^1, 2.18 × 10^2, 4.73 × 10^2, and 9.83 × 10^2 $\mu W/cm^2$. The photoreaction temperatures inside the filter holder were 24, 50, 60, and 70 °C.

2.2. AFR System. The second set of experiments involved establishment of the capture kinetics of Hg^0 in a flow reactor system (Figure 2B) similar to the one used by Wu et al.[2] A detailed description of in situ TiO_2 generation and the experimental procedure is given elsewhere.[2,14,15] The furnace (Lindberg, 1700 C single zone) aerosol reactor consisted of an alumina tube (91.44 cm length and 2.54 cm inner diameter). Titanium(IV) isopropoxide ($Ti[OCH(CH_3)_2]_4$; 97%, Aldrich) was used as a precursor for TiO_2. The photochemical reactor was 60 cm in length and 5 cm in inner diameter and was made of borosilicate glass (Pyrex, no. 7740). The transmittance of the borosilicate glass was 94% at 360 nm, 72% at 320 nm, and 30% at 300 nm. The UV lamp (Spectronics, type XX-40, 80 W) was 120 cm in length, and the intensity at 365 nm was 1.85 mW/cm^2 at a distance of 25 cm. The total flow rate of air through the system was fixed at 1 L/min, with flow rates of other gases listed in Table 1.

Metal screens of different meshes were used to vary the intensity of the incident light. A glass fiber filter (no. 61663, Gelman Science) was used downstream to collect particles for composition analyses. The elemental mercury concentration in the gas stream was monitored using the online mercury (Hg^0) analyzer. To measure the particle size distribution in real time, sampling ports were installed before and after the photochemical reaction cell to direct the sample particles to a scanning mobility particle sizer (model 3934 DMPS, TSI Inc.). The bottom half of the glass column was covered with heating tape for temperature variation, allowing UV light to penetrate through the top.

Table 1 shows the experimental plans and conditions. The inlet concentration of Hg ranged from 0.2 to 2.0 $\mu g/m^3$. The UV intensities measured inside the photochemical reaction cell were 1.28 × 10^2, 4.33 × 10^2, 1.14 × 10^3, and 2.56 × 10^3 $\mu W/cm^2$. The water vapor concentration was about 700 ppmv. The filter holder was covered first with aluminum foil and then with black cloth to ensure that the in situ generated TiO_2 particles were irradiated only while passing through the photochemical reaction cell. The temperatures inside the photochemical reaction cell were 24, 40, 50, 80, 110, and 130 °C. The photooxidation time (residence time under UV irradiation) ranged from 50 to 60 s, depending on the total flue gas flow rate. Glass fiber filters were equilibrated at a set humidity (20%) and weighed before and after the run without Hg in the system so that the total mass of TiO_2 participating in the heterogeneous reaction at a given residence time could be calculated. For the argon (titania precursor carrier gas) flow rate of 200−300 cm^3/min and the titanium isopropoxide bubbler temperature of 75−85 °C, the feed rate of TiO_2 was in the range of 1.0−10.0 $\mu g/s$.

3. Kinetic Model Equations

A qualitative mechanism for the capture of Hg on TiO_2 sorbents using UV irradiation has been proposed earlier.[2] Upon irradiation by UV light, active sites become available on the titania particle surface and the adsorbed mercury forms a complex with TiO_2 (Figure 1). The overall pathway is expressed as follows:

$$TiO_2(s) + UV \rightarrow TiO_2{\cdot}OH + Hg(g) \rightarrow TiO_2{\cdot}HgO(complex) \quad (1)$$

First, the kinetic data measured were fitted to the LH expression, and a negative value for the apparent adsorption constant, K, was obtained, a number that should always be positive.[7] Dibble and Raupp[9] reported that the integral rate law expression was superior to the LH or to the Langmuir−Hinshelwood−Hougen−Watson (LHHW) rate forms. The reason for the inapplicability of the LH model is discussed later in the Results and Discussion section. Hence, if x represents the fraction of TiO_2 that is associated with the mercury species, similar to the model proposed by Mahuli et al.,[10] the initial reaction rate is

$$dx/dt = k_{exp} A_{TiO_2}{}^{n} C_{Hg}{}^{\alpha} I_{UV}{}^{\beta} \quad (2)$$

where k_{exp} is the experimentally observed reaction rate constant, A_{TiO_2} is the available specific surface area of TiO_2 for adsorption, C_{Hg} is the gas-phase elemental

mercury concentration, and I_{UV} is the UV intensity. x was estimated as follows: First, the amount of Hg^0 captured for a fixed duration of time was calculated. Then, assuming a stoichiometric reaction, the amount of TiO_2 converted (associated with Hg) was calculated. Finally, when the mass of converted TiO_2 is divided by the initial amount of TiO_2 in the system, the fraction, x, was obtained. As the active sites get occupied by Hg species, they are no longer available for further adsorption. Furthermore, particles are solid (minimal intraparticle porosity) as they are generated at high temperatures,[18] and only the external surface is used for the reaction. Therefore, it can be assumed that $n = 1.0$, and the active surface area available for reaction is

$$A_{TiO_2} = S_o(1 - x) \tag{3}$$

where S_o is the total effective specific surface area of TiO_2. Equation 2 thus becomes

$$dx/dt = k_{exp} S_o (1 - x) C_{Hg}{}^{\alpha} I_{UV}{}^{\beta} \tag{4}$$

Because the experiments were conducted with constant C_{Hg} and I_{UV}, eq 4 was readily integrated to yield (with $x = 0$ at $t = 0$)

$$-\ln(1 - x) = k_{exp} S_o C_{Hg}{}^{\alpha} I_{UV}{}^{\beta} \Delta t \tag{5}$$

A plot of $-\ln(1 - x)$ versus C_{Hg} on a log−log plot would yield α as the slope. Similarly, a plot of $-\ln(1 - x)$ versus I_{UV} on a log−log plot yields β as the slope. Using these average values of α and β, the value of the experimentally observed rate constant, k_{exp}, can be calculated if the value of the effective specific surface area is known. The rate constant, k_{exp}, is expressed as follows:

$$k_{exp} = A \exp\left(\frac{-E_a}{RT}\right) = A \exp\left(\frac{-(E_s - \lambda)}{RT}\right) \tag{6}$$

where A is a preexponential factor, E_a is the apparent activation energy, E_s is the true activation energy for the surface reaction, and λ is the heat of adsorption. The value of E_a can be both negative and positive, depending on the values of E_s and λ.[19] Hence, it can also be used to identify which of the two processes, adsorption or surface reaction, is dominant in the temperature range tested. Reaction rates measured at various photoreaction temperatures would yield the value of k_{exp} as a function of temperature if the initial effective specific surface area, S_o, is known.

4. Results and Discussion

4.1. DBR System. Degussa P25 and the aerosol-route-generated TiO_2 were used in a DBR system in the presence of UV irradiation ($I_{UV} = 9.83 \times 10^2$ $\mu W/cm^2$). In Figure 3A, $-\ln(1 - x)$ versus C_{Hg} is plotted on a log−log scale for 0.001 g of Degussa P25 and 0.001 g of the aerosol-route-generated TiO_2. The reaction order, α, with respect to the inlet Hg concentration (determined from the slope) was 1.41 and 1.42 for aerosol-route-generated TiO_2 and Degussa P25, respectively. Both powders resulted in a statistically similar value of α (1.4 ± 0.1), the averaged value over several experiments at different UV intensities tested (1.28×10^2, 4.33×10^2, 1.14×10^3, and 2.56×10^3 $\mu W/cm^2$).

Next, photooxidation of Hg was measured at various UV intensities. The slope representing the reaction order with respect to the UV intensity varied according to the thickness of the titania powder layer spread over the filter. First, 0.001 g of Degussa P25 and the aerosol-route-generated TiO_2 was used in the DBR, and they were spread carefully to avoid overlayering. Though overlayering could only be avoided on a qualitative basis, this was done carefully to minimize this. When all of the TiO_2 particles are exposed to the UV light, the log−log plot of $-\ln(1 - x)$ versus I_{UV} yields a straight line, indicating that the oxidation of Hg has a linear dependence on the UV intensity (Figure 3B). Calculation of the slope by fitting the curves gives the β value of 0.35 ± 0.05, which is lower than the value of 0.7 ± 0.1 reported by Peral and Ollis[20] for photooxidation of acetone by TiO_2 and the theoretically calculated range of $0.5 < \beta < 1.0$.[20−22] The value of β is close to 0.5 for high-intensity UV light and close to 1.0 for low-intensity UV light. The two asymptotic values of β above were calculated using the electron−hole pair generation model, and the recombination of electron−hole pairs (consequently, a decrease in the activated sites) due to the large number of electron−hole pairs generated at high UV intensity was accounted for by the lower end value of β close to 0.5. In our case, the total number of activated sites on the titania surface was continuously decreasing because of the occupation of activated sites by the HgO molecules (chemical binding) as well as the recombination of electron−hole pairs caused by high UV intensity, while for other reported cases,[20,21] the product

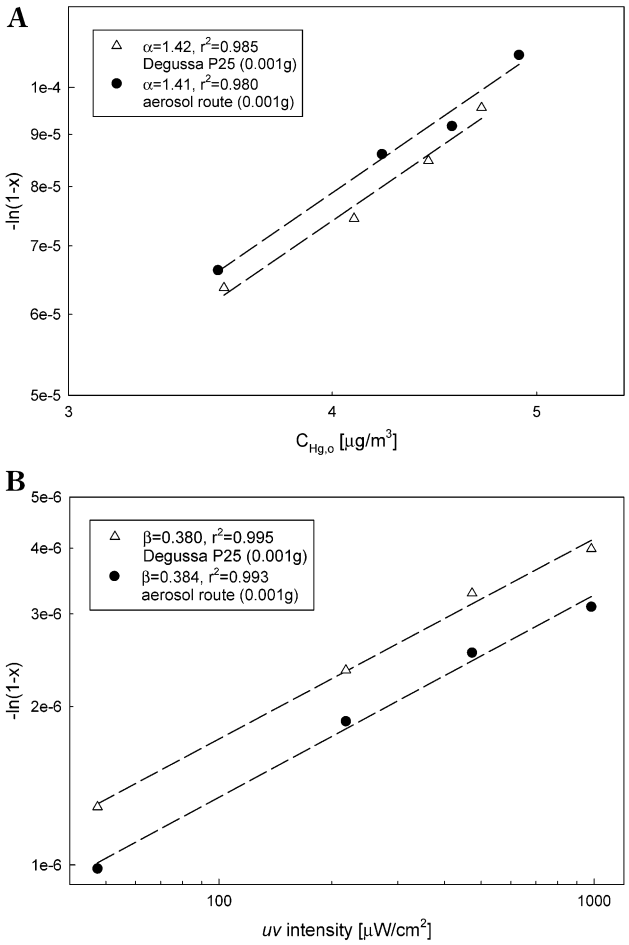

Figure 3. (A) Reaction order with respect to the Hg concentration (DBR system); $I_{UV} = 9.83 \times 10^2$ $\mu W/cm^2$. (B) Reaction order with respect to the UV intensity (DBR system); $C_{Hg,o} = 3.5 \pm 0.1$ $\mu g/m^3$.

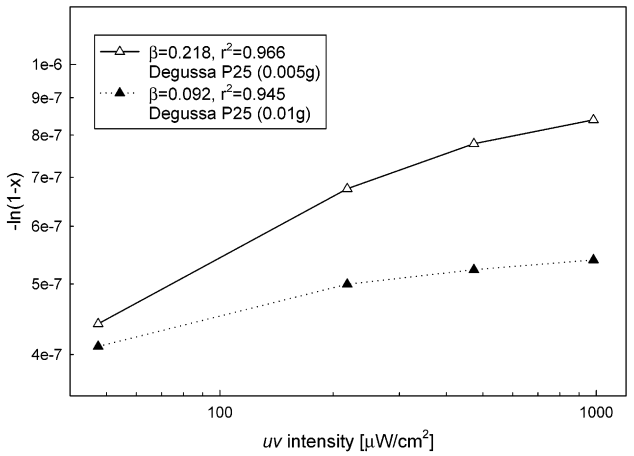

Figure 4. Reaction order with respect to the UV intensity (DBR system); $C_{Hg,o} = 3.5 \pm 0.1$ μg/m^3.

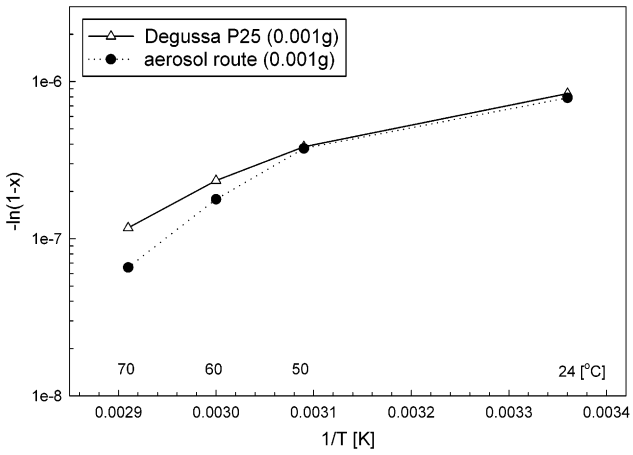

Figure 5. Reaction rate vs photoreaction temperature (DBR system); $C_{Hg,o} = 3.5 \pm 0.1$ μg/m^3 and $I_{UV} = 9.83 \times 10^2$ μW/cm^2.

species diffuse away from the active sites, making them available for the next reactant species. When a higher mass of TiO_2 powder was used, the particles formed a thicker layer on the filter and overlapping could not be avoided. As shown in Figure 4 (Degussa P25, 0.005 and 0.01 g), the curves flatten out as the intensity of UV light increases. This is because photons generated from the UV lamps can only penetrate a limited distance into the TiO_2 layer. In 1973, Courbon et al. (as cited in ref 20) reported that 99% of the light adsorption occurs within a TiO_2 anatase layer of 4.5 μm, which means that only TiO_2 particles up to this depth can be irradiated to activate the reaction sites. Calculated values of β range from 0.06 to 0.25, indicating that the reaction rate is proportional to the effective surface area for UV irradiation rather than to the total mass. This was validated by carrying out experiments using 0.001 g of Degussa P25 again. Only this time the powders were intentionally placed in multiple overlapping layers. β values were found to be 0.22 ± 0.02 with r^2 values of less than 0.98. This is important because it indicates that, although the DBR can minimize the mass-transfer resistance, it may have the limitation of UV light transport onto the surface of the photocatalyst. Therefore, extreme care has to be utilized to ensure that all of the particles are exposed to the incident light, and especially to establish the associated kinetic parameters for photocatalytic reactions.

The conversion (utilization of titanium dioxide) was measured at various photoreaction temperatures (24, 50, 60, and 70 °C) using the modified filter holder described earlier (Figure 2A). Degussa P25 and the aerosol-route-generated TiO_2 (0.005 g) were tested to investigate rate changes as a function of the temperature. Figure 5 is a plot of $\ln\{-\ln(1 - x)\}$ versus $1/T$, where T is the photoreaction temperature. From eqs 5 and 6, the slope is proportional to the apparent activation energy, E_a. The slope ($E_a < 0$) from Figure 5 indicates that adsorption is beginning to control the overall process for the DBR system in the temperature range tested ($E_s < \lambda$). The difference in the reaction rate decrease at higher temperatures is probably due to the difference in the adsorption characteristics onto the activated sites of the Degussa P25 and aerosol-route-generated powders. It is also reported that the active sites on a single titania particle may possess different degrees of surface reactivity.[23] Hence, different adsorption/surface reaction characteristics result in different rates of reaction, especially in the high-temperature region where both the heat of adsorption and the surface reactivity are more sensitive to temperature changes.

4.2. AFR System. An AFR was also used to study the same reaction. Flow reactor studies are more representative of the mercury-sorbent photocatalytic reaction that would occur in the entrained state in practical systems. No noticeable change of the gas-phase elemental Hg concentration in the flue gas was observed in the absence of UV irradiation in the photoreaction temperature range tested (24−130 °C), indicating that adsorption was minimally effective in the removal of Hg. The conversion of TiO_2, x, was measured at various feed rates of the titania precursor in the presence of UV irradiation. A plot of TiO_2 conversion versus inlet feed concentration of TiO_2 on a log−log plot (Figure 6A) shows that n, the reaction order with respect to the total surface area, is 0.97 ($r^2 = 0.997$), which is close to 1.0. Figure 6B shows the log−log plot of $-\ln(1 - x)\}$ versus C_{Hg}. The slope, α, is 1.1 ± 0.1, lower than the value (1.41) evaluated for the DBR system. It should be noted that the value obtained in the AFR is closer to 1 and, hence, may be more representative of a first-order reaction rate with respect to the inlet mercury concentration. The difference could also be due to inherent errors (as discussed earlier) in the DBR experiments.

The reaction order with respect to the UV intensity is shown in Figure 6C for the in situ generated titania particles. The β value is 0.39 ($r^2 = 0.987$), close but slightly higher than the values (0.35) found for the DBR system, indicating that the in situ generated TiO_2 particles in the AFR system utilize the available UV light more effectively than those in the DBR system.

Finally, the in situ generated TiO_2 was tested for its Hg oxidation capacity at various temperatures (24, 40, 50, 80, 110, and 130 °C) using a modified photochemical reactor (Figure 2B). Results are shown in Figure 7. In a lower temperature range, the overall rate of elemental mercury uptake by titania sorbent particles increases as the photoreaction temperature increases. In other words, the surface reaction is a dominant process in this temperature range. Decreases in the adsorption rates are overcome by enhanced reactivity of the mercury−titania particles. However, as the temperature is further increased (>110 C), the decrease in the concentration of absorbed Hg begins to control the overall process. Also, the rate of reactivity increase may slow as the temperature further increases because of the lower

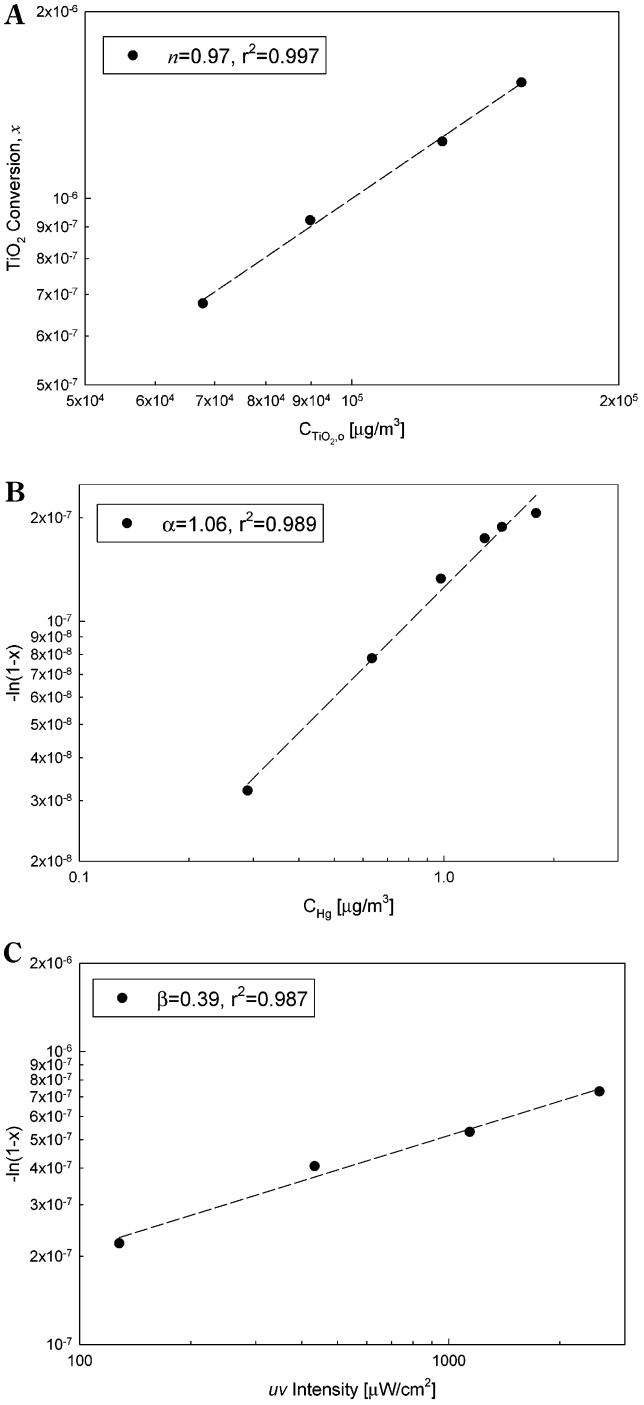

Figure 6. (A) Reaction order with respect to the inlet TiO_2 feed concentration (AFR system); $I_{UV} = 2.56 \times 10^3$ μW/cm^2. (B) Reaction order with respect to the Hg concentration (AFR system); $I_{UV} = 2.56 \times 10^3$ μW/cm^2. (C) Reaction order with respect to the UV intensity (AFR system); $C_{Hg,o} = 1.5 \pm 0.1$ μg/m^3.

adsorptivity of water molecules, which is critical for the formation of OH$^\bullet$ free radicals on the titania surface. The existence of such temperature maxima may explain the inapplicability of the LH model to this study because the LH model assumes that the number and activity of catalyst sites are constant with temperature.[20]

The experimentally observed rate constant, k_{exp}, is a function of the temperature (eq 6) and can be estimated if the initial effective specific surface area (S_o) is known. The BET surface area of the in situ generated TiO_2 (64.56 ± 0.5 m^2/g) may be used for S_o, although it is likely to be larger than the effective surface area, S_o. It

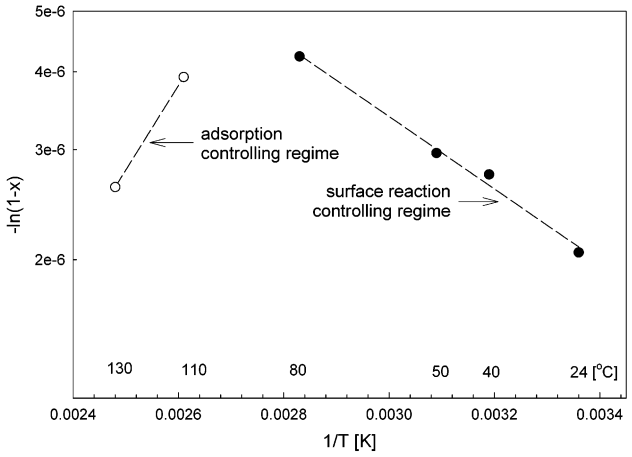

Figure 7. Reaction rate vs photoreaction temperature (AFR system); $C_{Hg,o} = 1.2 \pm 0.1$ μg/m^3 and $I_{UV} = 2.56 \times 10^3$ μW/cm^2.

is difficult to measure the effective surface area accurately because TiO_2 particles exhibit different morphology and size and, consequently, different values of S_o, depending on the titania precursor feed conditions.

5. Summary and Conclusions

The kinetics of photooxidation of Hg^0 by in situ generated TiO_2 was established by performing experiments in two reactors: differential bed and entrained-flow systems. No removal or capture of mercury is observed in the absence of UV irradiation, indicating that physical adsorption is not an effective pathway of capture for these inorganic sorbents. Results from the experiments performed at various photoreaction temperatures show that there are two regimes with different rate-controlling processes. In a positive E_a regime, as the temperature increases, the overall rate increases because of the fact that a reactivity increase offsets the decrease in adsorption ($E_s \gg \lambda$). In a negative E_a regime, adsorption outweighs the surface reaction.

A procedure of evaluating E_a and k_{exp} has been proposed, and it could be used to design sorbent capture processes for Hg capture. Using the value of k_{exp}, the amount of Ti precursor necessary for given Hg concentration levels at specific UV intensities can be estimated. The size of the in situ generated TiO_2 particle agglomerates can be readily controlled both to optimize the necessary surface area and to ensure that the resultant particles are captured in existing particle control devices.

Acknowledgment

The experimental work was done at University of Cincinnati and supported by the Ohio Coal Development Office (Grant OCRC-99-B4.7). Partial support provided by the U.S. EPA through an Internal Grant Research Project for chemical analysis of Hg is gratefully acknowledged.

Nomenclature

α = reaction order with respect to the gas-phase Hg^0 concentration
A = preexponential factor
A_{TiO_2} = specific surface area of TiO_2 available for adsorption (m^2/g)
β = reaction order with respect to the UV intensity

C_{Hg} = gas-phase Hg concentration ($\mu g/m^3$)
C_{TiO_2} = inlet feed concentration of TiO_2 ($\mu g/m^3$)
E_a = apparent activation energy (kJ/mol)
E_s = true activation energy for the surface reaction (kJ/mol)
I_{UV} = UV intensity ($\mu W/cm^2$)
k_{exp} = experimentally observed reaction rate constant
λ = heat of adsorption (kJ/mol)
S_o = total effective specific surface area of TiO_2 (m^2/g)
t = reaction time (s)
x = fraction of TiO_2 associated with the mercury molecule = (mass of captured Hg/MW_{Hg})(MW_{TiO_2}/mass of initial TiO_2)

Literature Cited

(1) Biswas, P.; Wu, C. Y. Control of Toxic Metal Emission from Combustors using Sorbents: A Review. *J. Air Waste Manage. Assoc.* **1998**, *48*, 113.

(2) Wu, C. Y.; Lee, T. G.; Tyree, G.; Arar, E.; Biswas, P. Capture of Mercury in Combustion Systems by *In Situ* Generated Titania Particles with UV Irradiation. *Environ. Eng. Sci.* **1998**, *15*, 137.

(3) Owens, T. M.; Biswas, P. Vapor Phase Sorbent Precursors for Toxic Metal Emissions Control from Combustors. *Ind. Eng. Chem. Res.* **1996**, *35*, 792.

(4) Owens, T. M.; Biswas, P. Reactions between Vapor Phase Lead Compounds and *In Situ* Generated Silica Particles at Various Lead−Silicon Feed Ratios: Applications to Toxic Metal Capture in Combustors. *J. Air Waste Manage. Assoc.* **1996**, *46*, 530.

(5) Biswas, P.; Zachariah, M. *In Situ* Immobilization of Lead Species in Combustion Environments by Injection of Gas Phase Silica Sorbent Precursors. *Environ. Sci. Technol.* **1997**, *31*, 2455.

(6) Larson, S. A.; Falconer, J. L. Characterization of TiO_2 Photocatalysts Used in Trichloroethene Oxidation. *Appl. Catal. B* **1994**, *4*, 325.

(7) Luo, Y.; Ollis, D. F. Heterogeneous Photocatalytic Oxidation of Trichloroethylene and Toluene Mixtures in Air: Kinetic Promotion and Inhibition, Time-Dependent Catalyst Activity. *J. Catal.* **1996**, *163*, 1.

(8) d'Hennezel, O.; Ollis, D. F. Trichloroethylene-Promoted Photocatalytic Oxidation of Air Contaminants. *J. Catal.* **1997**, *167*, 118.

(9) Dibble, L. A.; Raupp, G. B. Kinetics of the Gas−Solid Heterogeneous Photocatalytic Oxidation of Trichloroethylene by Near UV Illuminated Titanium Dioxide. *Catal. Lett.* **1990**, *4*, 345.

(10) Mahuli, S.; Agnihotri, R.; Chauk, S.; Ghosh-Dastidar, A.; Fan, L. S. Mechanism of Arsenic Sorption by Hydrated Lime. *Environ. Sci. Technol.* **1997**, *31*, 3226.

(11) Agnihotri, R.; Chauk, S.; Mahuli, S.; Fan, L. S. Selenium removal using Ca-based sorbents: Reaction kinetics. *Environ. Sci. Technol.* **1998**, *32*, 1841.

(12) Jadhav, R. A.; Agnihotri, R.; Gupta, H.; Fan, L. S. Mechanism of selenium sorption by activated carbon. *Can. J. Chem. Eng.* **2000**, *78*, 168−174.

(13) CFR, Title 40, Part 61, 1992.

(14) Lee, T. G. Study of Mercury Kinetics and Control Methodologies in Simulated Combustion Flue Gases. Ph.D. Thesis, Department of Civil & Environmental Engineering, University of Cincinnati, Cincinnati, OH, 1999.

(15) Lee, T. G.; Arar, E.; Biswas, P. Comparison of Mercury Capture Efficiencies of Three Different In Situ Generated Sorbents. *AIChE J.* **2001**, *47*, 954.

(16) Wu, C. Y.; Arar, E.; Biswas, P. Mercury Capture by Aerosol Transformation in Combustion Environments. Annual Meeting of the Air & Waste Management Association, Nashville, TN, 1996; Paper 96-MP2.02.

(17) Yang, G.; Zhuang, H.; Biswas, P. Characterization and Sinterability of Nanophase Titania Particles Processed in Flame Reactors. *Nanostruct. Mater.* **1996**, *7*, 675.

(18) Sahle-Demessie, E.; Gonzalez, M.; Wang, Z.; Biswas, P. Synthesizing Alcohols and Ketons by Photoinduced Catalytic Partial-Oxidation of Hydrocarbons in TiO_2 Film Reactors Prepared by Three Different Methods. *Ind. Eng. Chem. Res.* **1999**, *38*, 3276.

(19) Satterfield, C. N. *Heterogeneous Catalysis in Industrial Practice*, 2nd ed.; McGraw-Hill: New York, 1991.

(20) Peral, J.; Ollis, D. F. Heterogeneous Photocatalytic Oxidation of Gas-Phase Organics for Air Purification: Acetone, 1-Butanol, Butyraldehyde, Formaldehyde, and *m*-Xylene Oxidation. *J. Catal.* **1992**, *136*, 554.

(21) D'Oleivera, J.; Al-Sayyed, G.; Pichat, P. Photodegradation of 2- and 3-chlorophenol in TiO_2 aqueous Suspensions. *Environ. Sci. Technol.* **1990**, *24*, 990.

(22) Almquist, C.; Biswas, P. A Mechanistic Approach to Modeling the Effect of Dissolved Oxygen in Photo-oxidation Reactions on Titanium Dioxide in Aqueous Systems. *Chem. Eng. Sci.* **2001**, *56*, 3421.

(23) Garrone, E.; Bolis, V.; Fubini, B.; Morterra, C. Thermodynamic and Spectroscopic Characterization of Heterogeneity among Adsorption Sites: Carbon Monoxide on Anatase at Ambient Temperature. *Langmuir* **1989**, *5*, 892.

Resubmitted for review December 31, 2003
Revised manuscript received December 31, 2003
Accepted January 5, 2004

IE0303707